ELSEVIER

Thermochimica Acta 249 (1995) 351–366

thermochimica acta

A study of the porosity of water-plasticised polyacrylonitrile films by thermal analysis and microscopy

Duncan M. Price, Zahir Bashir*

Courtaulds plc, 101 Lockhurst Lane, Coventry CV6 5RS, UK

Received 24 June 1993; accepted 8 July 1994

Abstract

In a previous study, the morphology of water-plasticised polyacrylonitrile (PAN) film, made by compression moulding moist polymer powder, was discussed. The X-ray diffraction pattern of the plasticised film was different from that of dry PAN and this led to the suggestion that hydrated polymer crystallites had been formed by a portion of the water. The location of the remainder of the water was unknown. In this work, the thermal behaviour of the water-plasticised PAN at sub-ambient temperatures has been examined. When the film was cooled below room temperature, two distinct exothermic peaks were observed at −17°C and −38°C due to the formation of ice. By analysing the data in terms of thermoporometry, which has been more widely used to study the freezing of condensates in porous ceramic materials, it was concluded that the water-plasticised films had a micro-porous morphology. The DSC results suggested a bimodal distribution of pore sizes, but scanning electron microscopy revealed a third category of pores with larger size. These large pores were not detected by calorimetry because they were not fully filled with water.

Keywords: Bound-freezable water; DSC; Free water; Non-freezing water; Pore-size distribution; Thermoporometry; Water plasticized polyacrylonitrile

1. Introduction

Pure water does not dissolve or significantly swell polyacrylonitrile (PAN) at temperatures below its boiling point at atmospheric pressure. However, a 1984 Du Pont patent reveals that pure water dissolves PAN at temperatures above 180°C [1].

* Corresponding author.

0040-6031/95/$09.50 © 1995 – Elsevier Science B.V. All rights reserved
SSDI 0040-6031(94)01982-7

Subsequently, there was a series of American Cyanamid patents on the production of PAN fibres and films based on water-plasticised "melt extrusion" [2–8].

In the scientific literature, the first reports on the "melting" of PAN by water appears to be those of Frushour [9,10]. Experiments conducted in sealed, thick-walled glass tubes provided visual evidence that PAN powder does dissolve in water above about 180°C. Furthermore, differential scanning calorimeter (DSC) studies by Frushour demonstrated clear "melting" endotherms at about 180°C when PAN/water mixtures were heated; on cooling, crystallisation exotherms were observed. These results are unusual because on heating dry PAN (for example, powder or cast film), no melting endotherm is normally observed, unless exceptionally high heating rates are employed [11]. Thus, PAN is generally regarded as a polymer whose melting point is above its degradation temperature.

Our previous work showed that water-plasticised PAN films may be made by simply compression-moulding polymer powder which had been wetted with an appropriate amount of water [12]. These films had very different properties compared with films made by other methods such as solution-casting. For example, the water-plasticised films were different in appearance compared with cast films, being generally opaque. The films were also tough and flexible, and showed excellent ductility in the hydrated state. The X-ray diffraction pattern of the water-plasticised PAN film was also unusual [12]. In dry PAN powder, only two peaks with spacings of 5.3 and 3.0 Å are found. These have been attributed to a hexagonal polymorph. However, the water-plasticised films showed spacings of 10.0, 5.21, 5.10, 3.34, 3.03 and 2.90 Å which were attributed to the formation of an orthorhombic, hydrated polymorph. Infrared and Raman spectroscopy also suggested that water was hydrogen-bonded to the nitriles [12]. Thus, it was proposed that on cooling a high temperature PAN/water solution, the water was distributed in two different environments in the resulting film: a part of it co-crystallised with the polymer, thus giving the unusual diffraction pattern; the remainder was (assumed to be) held in the amorphous regions. The water existing in films made by this compression moulding method is metastable and evaporates if left unimmersed in water.

In this work, the thermal behaviour of water-plasticised PAN has been examined. Although Frushour described the high temperature behaviour (25–190°C), he did not report the sub-ambient properties. Here, the low temperature DSC transitions of these water-plasticised films are examined and a model for the morphology of the films is developed.

2. Experimental

2.1. Moulding of the water-plasticised film

Dry PAN powder was ground to a fine dust in a mortar. An equal weight of distilled water was added drop-wise with periodic grinding to distribute the water evenly. The porous powder was found to absorb the water by capillary action. The moist powder was placed between aluminium foil and held in a press at 210°C

under a pressure of 15 MPa. After 3 min, the press was rapidly cooled (under pressure) with circulating water and the sample removed when the press had cooled to room temperature. The moulded film was stored in distilled water prior to actual use, in order to inhibit dehydration. Before testing, samples were taken from the liquid and excess surface moisture was removed by blotting between filter paper.

The material obtained immediately after moulding contained 17% water and had a density of 1.05 g cm^{-3} (the density of dry PAN is 1.17 g cm^{-3} [13]). Samples of this were dried to various degrees in a domestic microwave oven. By controlling the power setting of the oven and the exposure times, it was possible to remove the water progressively, thus allowing films with different water contents to be prepared.

2.2. Thermal analysis

The water content of the as-prepared water-plasticised film was established by thermogravimetry using a Du Pont model 951 thermobalance and 9900 Computer Thermal Analyzer. A sample of film was heated to constant weight at 140°C under a stream of dry air (flow rate, 20 ml min^{-1}). The water content of the film is expressed as a weight percentage relative to the total mass of the sample. Subsequent water-content determinations were derived from weighings before and after controlled drying in the microwave oven.

Calorimetric measurements were carried out on each of the films containing different amounts of water using a Mettler DSC 30 and TC11 controller. Data storage and analysis were performed using an IBM microcomputer. The DSC cell was calibrated for temperature and enthalpy response according to the melting points and heats of fusion of freshly distilled mercury and water. The samples were encapsulated in hermetically sealed aluminium pans to minimise water loss. Each specimen was cycled twice between 30°C and −100°C at 4°C min^{-1}. The DSC curves were reproducible, and only the first cooling and heating cycles for each sample will be shown.

2.3. Scanning electron microscopy (SEM)

A Hitachi Field Emission microscope was used to obtain morphological information and to corroborate the conclusions reached by DSC.

3. Results

Fig. 1(a–f) shows a stacked plot of the cooling thermograms of a water-plasticised film after various degrees of drying. It can be seen that the samples with high water content show two or more overlapping peaks. For example, the undried film (a) with 17% total water shows two main crystallisation exotherms with peaks at about −17°C (peak I) and −38°C (peak II). As the sample was dried progressively, peak I disappeared first after removal of 8.55% water (d), followed

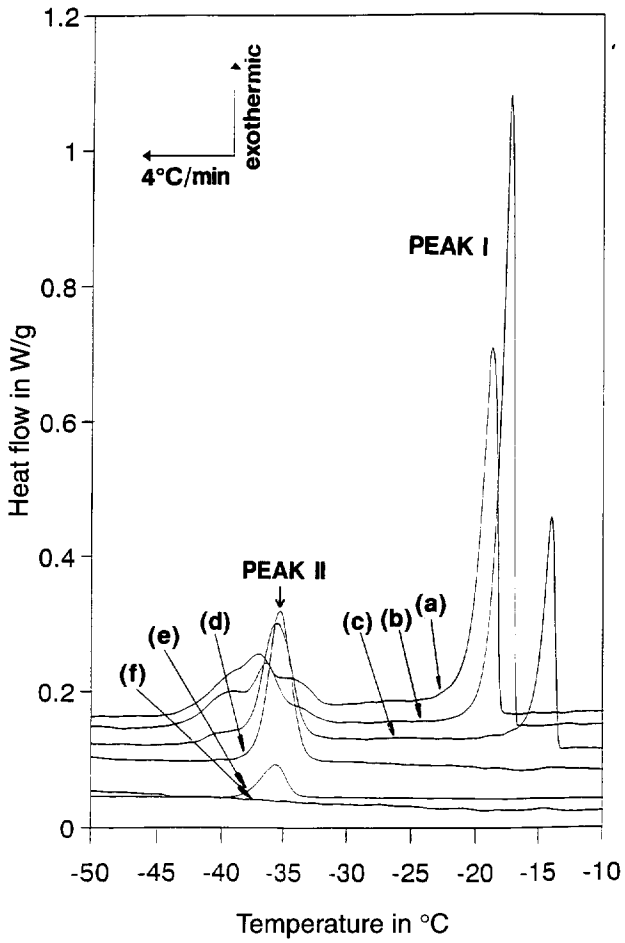

Fig. 1. Stacked plots showing DSC curves on cooling water-plasticised film as the water content was progressively reduced. The sequence shows percentage of water removed. (a) 0% (17% water percent), (b) 1.62%, (c) 5.45%, (d) 8.55%, (e) 12.67%, (f) 13.85%.

by peak II after the removal of 12.67% water (e). The remaining water was non-freezable (f) as no peaks were observed after 12.67% water had been removed. Interestingly, although the combined areas under peaks I and II decrease as the sample is dried, peak I of curve (b) has a higher enthalpy than the corresponding peak I of curve (a).

The heating thermograms (recorded after initial freezing) are shown in Fig. 2(a–f); the samples (a–f) are the same as the ones in Fig. 1(a–f) and hence these curves are complementary. Generally, the results obtained on heating show a hysteresis compared with those measured during cooling, and peaks I and II tend to merge.

The cooling behaviour of a 50% PAN powder/water blend, i.e. the moist powder before moulding, and dry PAN powder, are compared in Fig. 3.

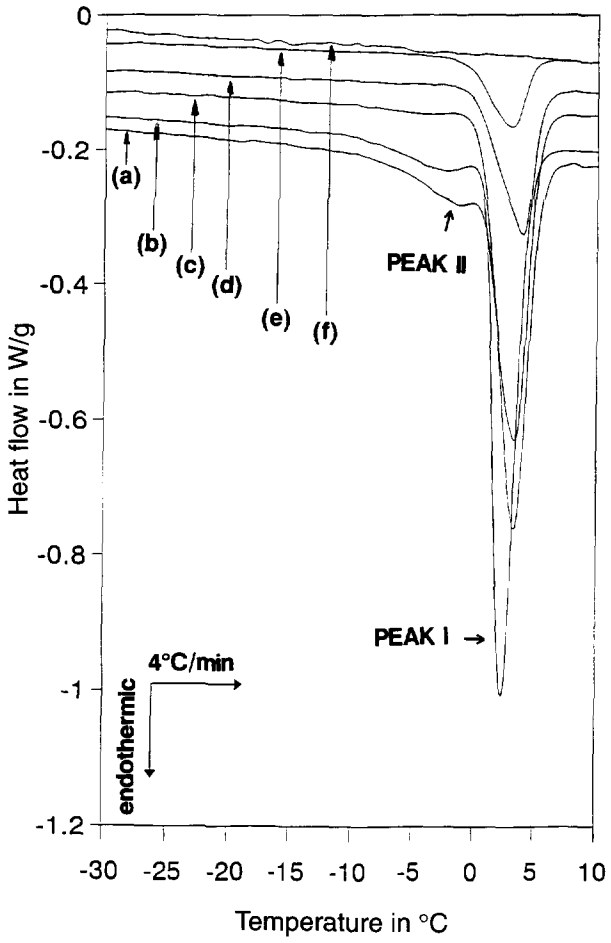

Fig. 2. Stacked plots of DSC curves obtained on heating the same samples as in Fig. 1. As before, the sequence shows the weight percentage of water removed. (a) 0%, (b) 1.62%, (c) 5.45%, (d) 8.55%, (e) 12.67%, (f) 13.85%.

Fig. 4 shows scanning electron micrographs of the morphology of the water-plasticised films. It can be seen that the plasticised film has a mosaic texture of fused powder particles and that there are voids with a typical diameter of 1 μm present, especially in the interior of the film.

4. Discussion

4.1. Categories of water in polymers

Water is a ubiquitous material that is present in the environment and hence there has been a considerable amount of work on the nature of the water absorbed in

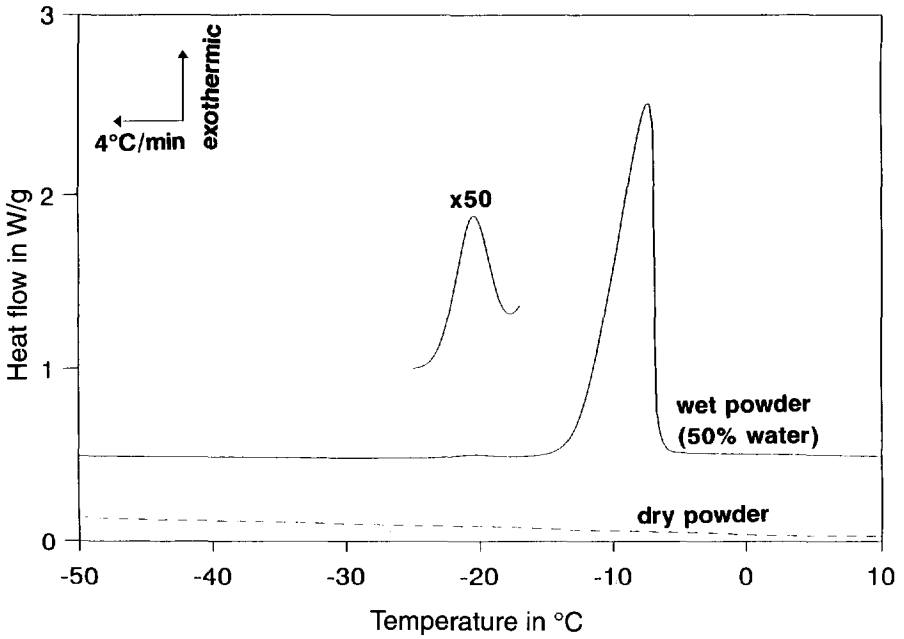

Fig. 3. DSC cooling curves of wet powder (50:50 PAN:water) and dry powder. There are two peaks in the wet powder. The inset shows a vertical expansion of the small peak at −20°C.

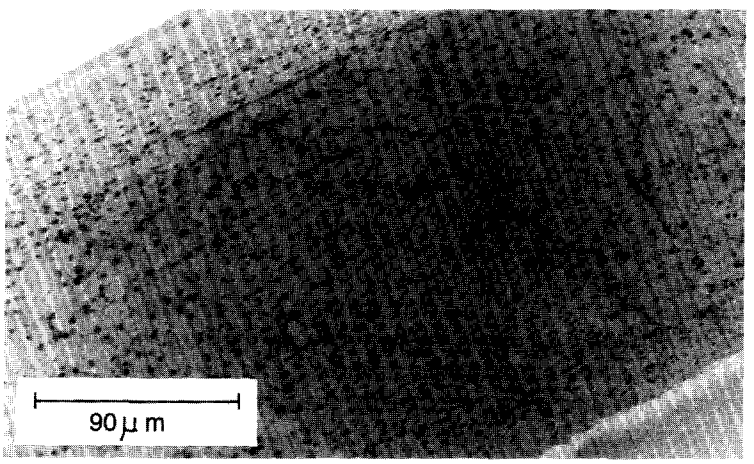

Fig. 4. SEM micrograph of the mosaic morphology and the presence of voids produced by the escape of steam. Cross section of film is shown.

polymers. Pertinent examples that may be cited are the studies on poly(vinyl alcohol) hydrogels [14–16], and on water absorbed in cellulose fibres [17–20] and polyacrylonitrile fibres [21], on the crystallisation of water in polyethylene oxide [22,23], as well as on the hydrogels and swollen membranes of other polymers such

as dextran, polyacrylamide and cross-linked poly(methyl methacrylate *N*-vinyl-2 pyrrolidone) copolymers [24–26].

Investigators in the polymer field often cite the existence of at least three categories of water: "free water" (water with the same freezing point as bulk water, i.e. near to 0°C), "freezable bound water" (water freezing at a temperature much lower than 0°C) and "non-freezing bound water" (water that does not form ice at all and therefore cannot be detected directly by calorimetry).

According to these classifications, it can be said that there is no free water in any of the PAN samples including the water-plasticised film containing 17% water. In contrast, Gref et al. [15] reported that lightly cross-linked poly(vinyl alcohol) hydrogels containing more than about 63% water showed a freezing peak near 0°C (in addition to other sub-zero peaks). PAN is not a water-soluble polymer like poly(vinyl alcohol) and hence it is not possible to make samples that can hold a similarly high quantity of water at room temperature, even in a metastable state.

The peaks I and II at −17°C and −38°C in Fig. 1 can be attributed to the second category, i.e. "freezable bound water". Note that for simplicity, we have just labelled two peaks; however, in Fig. 1(a–c), peak II appears to have several shoulders, so that it is actually made up of several overlapping peaks. Nakamura et al. [19] who studied the freezing of water absorbed in a variety of natural and man-made cellulose fibres showed DSC curves which are very similar to the ones in Figs. 1 and 2, though these involved oriented fibres impregnated with water in a different way, and hence were morphologically different from the plasticised film of this study. Work on poly(vinyl alcohol) hydrogels [14,15] also shows that, under certain circumstances, two (or even more) sub-ambient freezing peaks can arise.

In Nakamura et al.'s work [19], the highest temperature peak occurred in a similar temperature range to that of peak I here, but they chose to attribute this to free water rather than freezing bound water. Depending on the experimental conditions, pure bulk water often exhibits considerable supercooling, freezing a few degrees below 0°C. Evidence from the DSC curve of the moist PAN powder (Fig. 3) shows a 7–10°C supercooling for the excess free water. Thus peaks I and II in Fig. 1 can be attributed to freezable bound water, rather than to free water.

In non-polymeric materials, a similar depression of freezing point is observed in the freezing of water in porous ceramic materials such as alumina, clays, and concrete, and this has been related to the pore size [27]. "Thermoporometry" is thus a way of establishing the distribution of pore sizes in a material [27,28]. Although in the polymer literature, the freezing of water in systems such as poly(vinyl alcohol) hydrogels, and cellulose and PAN fibres is usually not interpreted explicitly with the concepts of thermoporometry, we shall apply this to analyse the freezing of water present in the plasticised PAN films.

4.2. Application of thermoporometry to interpret the DSC curves of the water-plasticised PAN films

Thermoporometry is a method devised by Brun and co-workers [27,28] which monitors the conditions of the solid–liquid phase transformation of a condensate

held inside a porous material. The conditions of equilibrium of the solid, liquid and gaseous phases of a pure substance which is highly dispersed are determined by the curvature of the interfaces. For a liquid contained in a porous material, the curvature of the solid–liquid interface depends closely on the pore size. The freezing temperature distribution is therefore dependent on the pore size distribution.

Thus, the solidification curve of a liquid inside a material of unknown porosity can be used to estimate the pore size distribution from the solidification temperature distribution. The volume of the pores can be computed from the heat involved in the phase transformation. Finally, by comparing the shapes of the freezing and melting thermograms, it is possible to obtain information on the shapes of the pores [27,28].

As with porous ceramic materials, in this work the freezing of water at temperatures substantially lower than 0°C in Fig. 1 can be interpreted as indicating the existence of a microporous morphology in the water-plasticised PAN film. The existence of two (or more) distinct crystallisation peaks was unexpected and suggests a bimodal (or multi-modal) distribution of pore sizes.

The key equations which allow the radius of curvature of the pore (R_p) and the distribution of pore volumes (dV/dR_p) to be obtained from the depression in melting temperature of water absorbed in pores (ΔT) and the calorimeter response (dQ/dt) are given below. Detailed derivation may be found in Brun and co-workers [27,28].

$$R_p = \frac{A}{\Delta T} + B \tag{1}$$

$$\frac{dV}{dR_p} = k \frac{\Delta T^2}{W_a} \frac{dQ}{dt} \tag{2}$$

for $0 > \Delta T > -40$°C.

In Eq. (1), $A = -64.67$ K nm and $B = 0.57$ nm. In Eq. (2), W_a is the heat of crystallisation of water and is given by the quadratic equation $W_a = -0.0556\Delta T^2 - 7.42\Delta T - 332$ J g^{-1}, and k is a constant given by $k = (m\, dT/dt\, \rho A)^{-1}$, where dT/dt is the cooling rate, m the mass of the sample, ρ its density (taken approximately as 1.0 g cm^{-3}) and A is as defined above.

Water thermoporometry is suitable for measuring pores with sizes in the range $2 < R_p < 65$ nm [27,28]. In fact, the definition of "freezable bound water" in the polymer literature could be made more precise by stating that this is freezable water existing in pores with radii between 2 and 65 nm. The distribution of pore sizes is obtained by plotting dV/dR_p versus R_p. The analysis is based on the assumption that the pores are fully saturated with the liquid.

Using this method, it is possible to estimate the average pore radius in the plasticised film from the equations given above. For peak I (at −17°C) in Fig. 1(a), this gives a pore radius of 3.6 nm. For peak II (at −38°C), $R_p = 2.3$ nm. As −17°C and −38°C are just the two peak temperatures in the DSC curves in Fig. 1(a), and the water actually freezes over a broad range of temperatures, there will be a distribution of pore radii.

Fig. 5(a) shows a plot of the pore radius distribution curve obtained from the DSC curve in Fig. 1(a). It can be seen that a bimodal distribution of pore sizes is

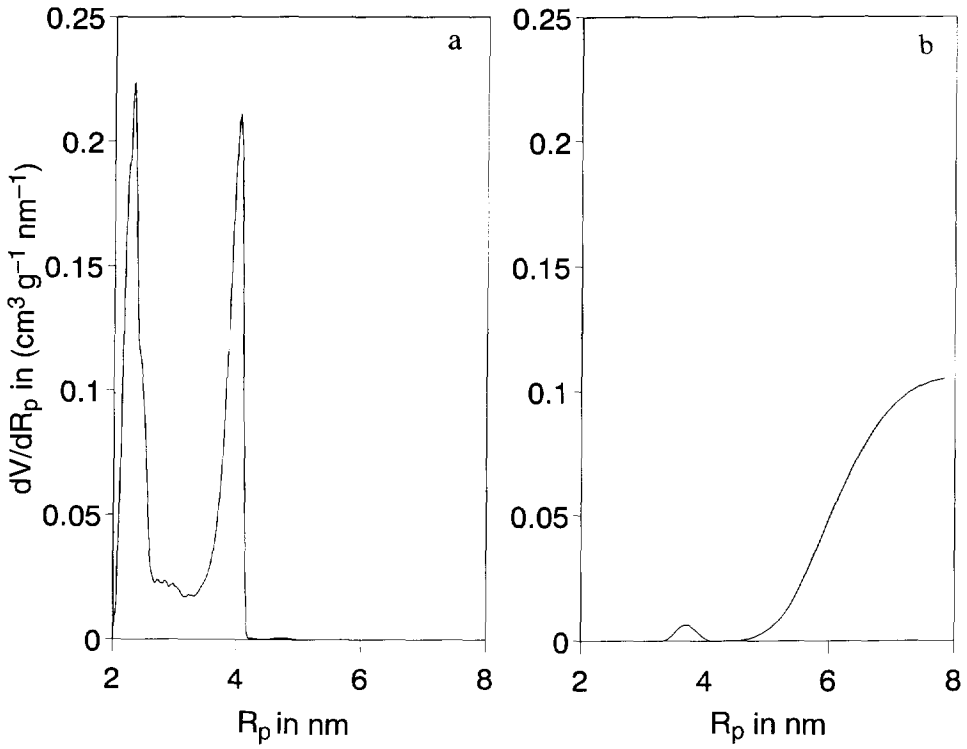

Fig. 5. Pore distribution curves dV/dR_p versus R_p: (a) film with 17% water; (b) 50:50 PAN:water powder.

obtained. On drying the film, peak I disappears before peak II, implying that water is removed preferentially from the large pores first. Pore size distribution curves may also be computed from the thermograms of the films from which the water was progressively removed (Fig. 1(b–f)); however, this would not yield representative information on the pore morphology as the probe (water) that was used to measure the pores was partially removed in these samples.

Thus, the DSC curves in Fig. 1 can be interpreted as indicating a pore morphology with a multi-modal distribution of pore sizes. Brun et al. [27] have shown that thermoporometry is sensitive enough to discriminate the presence of pores of two distinct sizes in a ceramic material that was made by mixing and sintering together two powders with different, but known, pore sizes. Other studies on the porosity of a Raney nickel catalyst as well as on ion exchange resins also appear to vindicate the theory [29].

It is pertinent to note the suitability of different condensates for thermoporometry. Benzene is also used because it undergoes a large decrease in the triple-point temperature, whereas water has the advantage that it has a high heat of crystallisation so that the presence of small voids is revealed. This work was not aimed at examining thermoporometry as a method of studying porosity; rather, the particular

method of fabrication of water-plasticised PAN film here lends itself to applying this technique to probe the resulting morphology. In a previous work, gel films of PAN with organic solvents such as ethylene carbonate and γ-butyrolacetone [30] were made by infiltrating the liquid into the porous polymer powder followed by compression moulding. However, the freezing behaviour of these condensates in the plasticised gel films did not lead to very distinct, well-resolved low temperature peaks, most probably because the heat of crystallisation of these liquids is much lower than that of water.

4.3. Void morphology of the plasticised film observed by SEM

The question arises as to how a micro-void morphology could arise in these films. The powder produced by slurry polymerisation of acrylonitrile is very porous. This powder is saturated with water (by capillary action) and compression moulded. On moulding at 210°C, the water dissolved the polymer. However, in the timescale of the moulding (about 5 min), it would appear that complete homogenisation did not occur as the water dissolved each powder particle from the outside. This would have led to concentration gradients with a higher level of water in the boundaries between the original powder particles and less water in the core of the particle. Note that in the continuous extrusion of water–PAN mixtures with a screw extruder, better homogenisation can be expected compared with compression moulding because of the high shearing present. Compression moulding is similar to the sintering process used by Brun and co-workers with inorganic ceramics; the difference in our case is that the condensate was added to the powder before compaction and, moreover, the liquid was capable of dissolving the powder under the processing conditions.

Fig. 4 shows a freeze-fractured cross-section of the film. This indicates that the film consists of semi-fused particles with the boundaries giving it a mosaic-like texture. Also evident is the presence of voids typically 1 μm in diameter, which appear to be concentrated in the interior of the film. These voids are much larger than that deduced from thermoporometry. Had voids of this size been fully filled with liquid, the latter would have behaved like bulk water and a third crystallisation exotherm with a peak between -10°C and 0°C would have occurred. This was not observed which suggests that these voids were mostly empty. The most probable cause for these large voids is the production of steam during moulding. The evaporation of water as steam during water-plasticised melt spinning of PAN is always problematic as it leads to some voiding of the fibres [31,32]. Thus both batch and continuous processes using water plasticisation lead to a certain degree of voiding.

The peak at -17°C in Fig. 1 probably arises from the water trapped in the regions between the boundaries of the original powder particles. According to theory, the average radius of curvature for this peak is about 4 nm. The microscope pictures could not resolve the presence (or absence) of pores of such sizes. One possible area where water could be trapped is the inter-particle zones shown in Fig. 4. However, these areas are about 100 nm in width, which is about 25 times the pore size deduced from thermoporometry. It is possible that there are pores with

radii of 4 nm which were not detectable by microscopy; alternatively, peak I in the curves of Fig. 1 could arise because there is a small amount of water in larger, but partially filled pores, and application of these equations to a partially filled system gives a distorted picture of the pore size (this might explain why in Fig. 1 peak I, curve (b) is bigger than peak I, curve (a)). Thus, there is a certain amount of ambiguity in deciding the origin and the true sizes of the pores responsible for the ice peak I in Fig. 1.

From thermoporometry, peak II at −38°C corresponds to an average pore radius of about 2 nm. Although there is no microscopic evidence, it seems reasonable to attribute this to the water trapped in the amorphous regions linking hydrated polymer crystallites as this is the typical dimension of voids or spaces between chains. The existence of PAN–water crystallites was inferred from X-ray diffraction and it would be reasonable to assume that water is also present in amorphous regions between crystallites. Unfortunately, practical considerations make it difficult to study water-filled pores of this dimension by visual means, as it would require transmission electron microscopy and the cutting of thin sections without losing the water during preparation.

4.4. *The heating curves of the water-plasticised PAN film*

If the cooling curve of the as-moulded film containing 17% water is compared with the heating curve obtained on warming the sample back to room temperature (Fig. 2(a)), it can be seen that in the latter there are two melting peaks, but they overlap when compared with the freezing peaks. This was always found to be the case. In the heating curves in which 5.45% water was removed (Fig. 2(c)), two peaks cannot be resolved. Brun et al. also demonstrated a similar deviation between the cooling and the heating thermograms of sintered alumina and sintered NiF_2 which had been filled with a condensate [27].

Although a similar phenomenon has also been shown in cooling and heating thermograms of other polymer–water systems such as poly(vinyl alcohol) hydrogels [14] and water-swollen cellulose and PAN fibres [19,21], its cause has not been discussed in the polymer literature. However, Brun and co-workers' analysis predicts the general conditions where such a behaviour will be observed [27].

During the freezing of the liquid in a spherical pore, the formation of the solid phase takes place from a spherical nucleus whose curvature is equal to twice the reciprocal of the radius of the pore. The freezing temperature therefore depends on the radius of the pore. During melting, the analysis is more complicated. If the pore is spherical, the curvature of the frozen condensate remains the same when fusion occurs as it was when solidification took place, and so the fusion and solidification temperatures should be the same. If the pore is cylindrical, the spherical nucleus grows spontaneously and adopts the shape of the pore; the curvature of the solid condensate now becomes equal to the reciprocal (rather than twice the reciprocal) of the radius and this affects its melting properties.

Thus, in the case of freezing, the relationship between the pore radius and the depression of the freezing point (Eq. (1)) can be written as $R_p = f(\Delta T_f)$; when fusion

takes place, it will be of the form $R_p = 0.5f(\Delta T_m)$, the function f being identical in both cases [27,28]. The analysis therefore predicts a hysteresis between the freezing and fusion curves when pores are not spherical. Whereas there is no ambiguity in obtaining the pore radius distribution curve, $dV/dR_p = f(R_p)$, from the freezing curve, it would be necessary to know in advance the shape of the pores in order to deduce a distribution function from the fusion curve [27,28].

Brun et al. [27] indicate how the difference between the freezing and fusion thermograms can be used to find the shape of the pores. In fact, actual pores are neither purely spherical nor purely cylindrical. However, they show that a porous material may be modelled by assuming it to be made up of a combination of spherical and cylindrical pores.

It is not intended to analyse the shape of the pores, as this does not shed any additional insight on the plasticised film. Following Brun and co-workers' model, it will be noted that the difference in peak shapes and positions between the cooling and heating curves in Figs. 1(a) and 2(a) of the same film, for example, indicate that the pores are not perfectly spherical.

4.5. Appearance and mechanical properties of water-plasticised PAN film

The presence of micro-voids containing water would not have been suspected on the basis of the visual appearance of the film and its mechanical properties alone; it was in fact the freezing behaviour of the water that led us to consider the existence of film porosity. Most materials, if porous and rigid, tend to be brittle (for example, sintered alumina, whether filled with air or water, is brittle). Freshly moulded water-plasticised PAN film is tough despite being micro-porous. For example, a 100 μm thick film could be bent back on itself without breaking. In the previous work, it was shown that these films could be drawn smoothly [12]. Clearly the water is not merely an inert liquid held in the pores but affects the mobility of the polymer molecules and therefore its mechanical properties. The metastable water in the film influences its mechanical properties, for if the film was allowed to dehydrate by leaving on the bench, it became brittle like other hard, porous solids, and could not be bent (even slightly) without snapping.

The opaque appearance of the water-plasticised film is also consistent with the morphology deduced from the DSC and SEM results. In contrast, when PAN films are cast from dimethyl sulphoxide solution, the films are generally transparent, both before and after drawing. In the water-plasticised film, it is the powder particles (rather than the voids) that are comparable in dimensions to the wavelength of light (400–800 nm) and therefore responsible for the light scattering. This interpretation is consistent with the dimensions of the power particles whose boundaries can be seen in Fig. 4.

4.6. Freezing behaviour and morphology of moist PAN powder

The DSC curve in Fig. 3 of the PAN powder–water mixture (before moulding) is also instructive. There are two exothermic peaks, with peak I at -7°C and peak

II at −20°C (vertically expanded inset). Here peak I is almost certainly due to the freezing of "free water", the 7°C depression being caused by supercooling which is also shown by bulk water. Thus, the pores of the powder are relatively large compared with the pores in the water-plasticised film, and the water that it contains is closer to bulk water than that present in the film. However, the small peak II at −20°C in Fig. 3 (inset) is similar to peak I in the film (Fig. 1(a)). This suggests that even before compression moulding there are some pores with radii of about 4 nm in the powder.

Fig. 5(b) shows the pore distribution curve of the powder derived from the DSC curve in Fig. 3. Comparing this with the curve in Fig. 5(a) (the plasticised film containing 17% water), it can be seen that the pores in the powder before compression moulding are, in general, larger (5 nm or greater) than in the film and their distribution is broader, but there is a detectable small population of very small pores with radii less than 4 nm. Note that for comparison with Fig. 5(a), the abscissa in Fig. 5(b) is truncated at 8 nm but the curve extends beyond 60 nm (which is the limit of water thermoporometry) as a distribution of pores up to 1 μm sizes is present in the powder. This was also evident when the powder was examined under the electron microscope.

4.7. *The non-freezing water in the film*

After the removal of about 12.7% water, there was no more freezable water (Fig. 1(f)). Because the initial film contained 17% water, we conclude that non-freezing water amounts to about 4.3%. This water must be associated with the nitrile groups on the polymer, and a substantial portion of this will be responsible for the hydrated crystallites previously proposed from X-ray studies on the films containing the full 17% water [12]. It was found that the samples with 4.3% water still showed the unusual X-ray pattern of the hydrated polymorph, and it was only when this water was dried out completely that the normal X-ray pattern of PAN was obtained.

It is worth comparing the maximum levels of non-freezable water in other polymers which have functional groups with affinity for water. In the case of the PAN film, these results indicate that the water content has to be in excess of 4.3% before it becomes freezable; for poly(vinyl alcohol) [14] and cellulose [19] these levels are about 19% and 20% by weight respectively. The level of water uptake depends on the degree of crystallinity of the polymer under consideration [14,19], as the water preferentially swells the amorphous regions. The values cited for polyvinyl alcohol and cellulose are taken from the literature but they may not be directly comparable because they do not compare water uptake at the same level of crystallinity.

However, there should also be intrinsic differences in the amount of water uptake between these different polymers. PAN is the least hydrophilic of the three polymers as only one water molecule per monomer unit can be hydrogen bonded (at the nitrile site). For poly(vinyl alcohol), two water molecules may be accommodated per monomer unit at every hydroxyl, as oxygen has two lone pairs, and hence

more non-freezable water may be absorbed in the amorphous regions during swelling. Cellulose has three hydroxyls and two ether-oxygen atoms per monomer unit, hence a greater amount of water can be absorbed in the amorphous regions, and only after these sites have been hydrated does any extra water become available for freezing.

It must be made clear that the normal uptake of moisture by PAN fibres is less than 1% under ambient conditions and even the 4.3% non-freezing water present in these films belongs to a metastable category, as much of this water evaporates if the film is left in the open. In contrast, cross-linked poly(vinyl alcohol) or cellulose fibres and films may be swelled to such an extent that they can take up more than 20% water under ambient conditions. Our water-plasticised PAN films had an unusually large water content only because of the exceptional way it was made: the polymer was dissolved in water at very high temperature and pressure, and was then cooled before the pressure was released. It is unlikely that such a water-plasticised film could be produced in a continuous process because water-plasticised melt extrusion leads to complete evaporation of the water during drawing and wind-up.

5. Conclusions

Compression moulding of moist PAN powder gave a smooth film, which was opaque and flexible, and which was entirely different from PAN films made by casting from solution. The water-plasticised films used in this study contained 17% by weight of water after moulding. The material had a complex morphology when viewed at different dimensional levels.

(a) From previous X-ray, infrared and Raman work, it was concluded that hydrated polymer crystallites were formed [12]. However, only a fraction of the water is actually involved in the crystallites. This may be termed "ordered water" and it would be non-freezable. From the present DSC results, this water would amount to 4.3% or less. The remainder (about 12.7%) may be termed disordered water and much of this would be observable as "freezing bound water".

(b) However, the DSC results indicate that the disordered water freezes in two distinct temperature ranges, with crystallisation peaks at $-17°C$ and $-38°C$. This was interpreted by applying the concepts of thermoporometry as indicating the presence of a microporous morphology with a bimodal distribution of pores. Pore size distributions were computed from the cooling thermograms.

(c) The $-17°C$ peak is associated with water crystallising in larger pores. The average radius of the associated pores calculated from thermoporometry is 3.6 nm. Pores of this size could not be corroborated independently by microscopy. This peak may be due to water trapped in the channels of the inter-particle boundary zone left after compression moulding of the water-filled powder.

(d) The $-38°C$ peak is most likely to be associated with the water freezing in the amorphous regions linking hydrated crystallites and corresponds to voids between chains. The average radius of the pores calculated for this peak from thermoporometry is 2.3 nm. Pores of this size could not be detected by SEM.

(e) There were larger pores with a typical diameter of 1 μm which could be detected by SEM, but not by DSC, suggesting that these voids were empty (or nearly empty) of water.

(f) Microscopy showed that the water-plasticised films had a mosaic texture due to the fact that the boundaries of the fused powder particles could still be seen. However, this did not lead to a brittle film, but it was consistent with the opaque nature of the films.

The present results show that the morphology of the water-plasticised PAN film made by moulding is more complex than originally thought. The water exists in several distinguishable environments: freezable water in pores of possibly two or three distinct sizes, and non-freezable water that has co-crystallised with the polymer.

In this work, a thermoanalytical technique, DSC, has been a useful morphological probe. Microscopy is often the dominant tool in such investigations, but in this instance, the in situ detection of sub-micron pores would have been difficult by microscopy as sample preparation would have caused damage. Thermoporometry has been used more with ceramic and other porous materials. It does not seem to have been applied widely to the analysis of pores in polymers, though its use has been recognised by membrane technologists [33]. It is hoped that this paper will spread the use of thermoporometry to the study of polymer hydrogels.

References

[1] C.D. Coxe, US patent 2,585,444 (1948, Du Pont).
[2] H. Porosoff, US patent 4,163,770 (1979, American Cyanamid).
[3] C.C. Young and F. De Maria, US patent 4,283,365 (1961, American Cyanamid).
[4] C.C. Young and F. De Maria, US patent 4,379,113 (1983, American Cyanamid).
[5] F. De Maria and C.C. Young, US patent 4,303,607 (1981, American Cyanamid).
[6] C.C. Young and F. De Maria, US patent 4,461,739 (1984, American Cyanamid).
[7] M.M. Zwick, US patent 4,301,112 (1981, American Cyanamid).
[8] G.K. Klausner, R.P. Kreahling and V.T. Sinha, US patent 3,991,153 (1976, American Cyanamid).
[9] B.G. Frushour, Polym. Bull., 4 (1981) 305.
[10] B.G. Frushour, Polym. Bull., 7 (1982) 1.
[11] P. Dunn and B.C. Ennis, J. Appl. Polym. Sci., 14 (1970) 1795.
[12] Z. Bashir, S.P. Church and D. Waldron, Polymer, 35 (1994) 967.
[13] H. Rein, Angew. Chem., 61 (1949) 242.
[14] T. Hatakeyama, A. Yamauchi and H. Hatakeyama, Eur. Polym. J., 20 (1984) 61.
[15] R. Gref, Q.T. Nguyen, J. Rault and J. Neel, Eur. Polym. J., 28 (1992) 1007.
[16] A. Higuchi and T. Iijima, Polymer, 26 (1985) 1207.
[17] T. Hatakeyama, Y. Ikeda and H. Hatakeyama, Makromol. Chem., 186 (1987) 1875.
[18] R.A. Nelson, J. Appl. Polym. Sci., 21 (1977) 645.
[19] K. Nakamura, T. Hatakeyama and H. Hatakeyama, Text. Res. J., 51 (1981) 607.
[20] C.E. Boesen, Cellul. Chem. Technol., 4 (1970) 149.
[21] T. Hori, H.-S. Zang, T. Shimizu and H. Zollinger, Textile Res. J., 58 (1988) 227.
[22] M.J. Hey and S.M. Ilett, J. Chem. Soc. Faraday Trans., 87 (1991) 3671.
[23] M.J. Hey and S.M. Ilett, J. Chem. Soc. Faraday Trans., 86 (1990) 2673.
[24] A. Takazawa, T. Kinoshita, O. Nomura and Y. Tsujita, Polym. J., 17 (1985) 747.
[25] M. Shibikuwa, N. Ohta and N. Onda, Bull. Chem. Soc. Jpn., 63 (1990) 3490.

[26] A.B. Ahmad and M.B. Huglin, Polym. Int., 33 (1994) 272.
[27] M. Brun, A. Lallemand, J.-F. Quinson and C. Eyraud, Thermochim. Acta, 21 (1977) 59.
[28] M. Brun, J.-F. Quinson and C. Eyraud, L'actualité chimique, October 1979, pp. 21–26.
[29] M.-J. Luys and P.H. van Oeffelt, DSM Publ. B0712, DSM Research, Geleen, The Netherlands.
[30] Z. Bashir, S.P. Church and D.M. Price, Acta Polym., 44 (1993) 211.
[31] D. Grove, P. Desai and A.S. Abhiraman, Carbon, 26 (1988) 403.
[32] B.G. Min, T.W. Son, B.C. Kim and W.H. Jo, Polym. J., 24 (1992) 841.
[33] M. Mulden, Basic Principles of Membrane Technology, Kluwer Academic Publishers, Dordrecht, The Netherlands, 1991, p. 126.